Synthesis and Characterization of Water-Soluble Silver(I) Complexes with L-Histidine (H_2his) and (*S*)-(−)-2-Pyrrolidone-5-carboxylic Acid (H_2pyrrld) Showing a Wide Spectrum of Effective Antibacterial and Antifungal Activities. Crystal Structures of Chiral Helical Polymers $[Ag(Hhis)]_n$ and $\{[Ag(Hpyrrld)]_2\}_n$ in the Solid State

Kenji Nomiya,*,† Satoshi Takahashi,† Ryusuke Noguchi,† Satomi Nemoto,† Toshio Takayama,‡ and Munehiro Oda§

Department of Materials Science, Faculty of Science, Kanagawa University, Hiratsuka, Kanagawa 259-1293, Japan, Department of Applied Chemistry, Faculty of Engineering, Kanagawa University, Rokkakubashi, Yokohama, Kanagawa 221-8686, Japan, and Meiji Cell Technology Center, Meiji Milk Products Co., 540 Naruda, Odawara, Kanagawa 250-0862, Japan

Received May 14, 1999

Two water-soluble, silver(I) complexes showing a wide spectrum of effective antibacterial and antifungal activities, i.e., $\{[Ag(Hhis)]\cdot 0.2EtOH\}_2$ (**1**; H_2his = L-histidine) and $[Ag(Hpyrrld)]_2$ (**3**; H_2pyrrld = (*S*)-(−)-2-pyrrolidone-5-carboxylic acid) were prepared. In aqueous solution **1** and **3** were present as dimers, whereas in the solid state they were polymers. Crystallization of **1** by slow evaporation and/or vapor diffusion gave water-insoluble crystals of $[Ag(Hhis)]_n$ (**2**) showing modest antimicrobial activities. The complex **1** in the solid state is a polymer formed by intermolecular hydrogen-bonding interactions between dimeric $[Ag(Hhis)]_2$ cores, while **2** is a different polymer without a core complex. X-ray crystallography revealed that **2** was a left-handed helical polymer consisting of a bent, 2-coordinate silver(I) atom bonding to the N_{amino} atom of one $Hhis^-$ ligand and the N_π atom of a different $Hhis^-$ ligand. Of particular note is the fact that $O_{carboxyl}$ atoms do not participate in the coordination. X-ray crystallography also revealed that **3** was a left-handed helical polymer formed by self-assembly of dimeric $[Ag(Hpyrrld)]_2$ cores with an intramolecular metal(I)−metal(I) interaction (Ag−Ag distance, 2.9022(7) Å). The FT-IR and the solid-state ^{13}C and ^{15}N NMR spectra showed that the dimeric core of **1** was formed through Ag−N bonds, while that of **3** was formed through Ag−O bonds. The molecular ions of **1** and **3** were detected by the positive-ion electrospray ionization (ESI) mass spectrometry. For **1**−**3**, characterization by elemental analysis, TG/DTA, FT-IR, and variable-temperature solid-state ^{13}C NMR and room-temperature ^{15}N NMR measurements was performed, and for **1** and **3**, that by solution molecular weight measurements and solution (^{109}Ag, ^1H, and ^{13}C) NMR spectroscopies was also carried out. The antibacterial and antifungal activities of **1** and **3** were remarkable and comparable to those of the previous silver(I)−N-heterocycle complexes.

Introduction

In bioinorganic chemistry of coinage metal(I) complexes, there have been only a few biological and medicinal studies of silver(I) complexes, in comparison with many studies of gold(I) complexes. The studies of silver(I) complexes have been mostly related to their antiethylene[1] and antimicrobial activities,[2] and those of gold(I) complexes, mostly to their antiarthritic,[3] antitumor,[3a,b,4] and also, recently, antimicrobial activities.[5] We have been interested in the structure−activity correlation of the coinage metal(I) complexes.[6]

One recently highlighted topic in the coordination chemistry of coinage metal(I) atoms is the d^{10}−d^{10} interaction between two closed-shell cations, or the aurophilic interaction, many examples of which have been recently reported and reviewed in gold(I) and silver(I) complexes.[7−9] The weak gold(I)−gold-

* Corresponding author. Fax: +81 463/58-9684. E-mail: nomiya@chem.kanagawa-u.ac.jp.

† Department of Materials Science, Kanagawa University.

‡ Department of Applied Chemistry, Kanagawa University.

§ Meiji Milk Products Co.

(1) (a) Veen, H.; Kwakkenbos, A. A. M. *Sci. Hortic. (Amsterdam)* **1982**, **1983**, *18*, 277. (b) Veen, H. *Sci. Hortic. (Amsterdam)* **1983**, *20*, 211.

(2) (a) Thurman, R. B.; Gerba, C. P. *CRC Crit. Rev. Environ. Control* **1989**, *18*, 295. (b) Lopez-Garzon, R.; Romero-Molina, M. A.; Navarrete-Guijosa, A.; Lopez-Gonzalez, J. M.; Alvarez-Cienfuegos, G.; Herrador-Pino, M. M. *J. Inorg. Biochem.* **1990**, *38*, 139. (c) Davies, K. M.; Hobson, G. E.; Grierson, D. *Plant Cell Environ.* **1988**, *11*, 729.

(3) (a) Shaw, C. F., III *Chem. Rev.* **1999**, *99*, 2589. (b) Shaw, C. F., III *Uses of Inorganic Chemistry in Medicine*; Farrell, N. P., Ed.; RSC: London, UK, 1999; Chapter 3, p 26. (c) Kaim, W.; Schwederski, B. *Bioinorganic Chemistry: Inorganic Elements in the Chemistry of Life*; John Wiley: New York, 1994; p 373. (d) Abrams, M. J.; Murrer, B. A. *Science* **1993**, *261*, 725. (e) Corey, E. J.; Mehrotra, M.; Khan, A. U. *Science* **1987**, *236*, 68. (f) Elder, R. C.; Eidsness, M. K. *Chem. Rev.* **1987**, *87*, 1027.

(4) (a) Parish, R. V. *Interdiscip. Sci. Rev.* **1992**, *17*, 221. (b) Sue, R. J.; Sadler, P. J. *Met.-Based Drugs* **1994**, *1*, 107. (c) de Vos, D.; Clements, P.; Pyke, S. M.; Smyth, D. R.; Tiekink, E. R. T. *Met.-Based Drugs* **1999**, *6*, 31. (d) McKeage, M. J.; Papathanasiou, P.; Salem, G.; Sjaarda, A.; Swiegers, G. F.; Waring, P.; Wild, S. B. *Met.-Based Drugs* **1998**, *5*, 217. (e) Berners-Price, S. J.; Sadler, P. J. *Coord. Chem. Rev.* **1996**, *151*, 1. (f) Berners-Price, S. J.; Mirabelli, C. K.; Johnson, R. K.; Mattern, M. R.; McCabe, F. L.; Faucette, L. F.; Sung, C.-M.; Mong, S.-M.; Sadler, P. J.; Crooke, S. T. *Cancer Res.* **1986**, *46*, 5486.

(5) (a) Novelli, F.; Recine, M.; Sparatore, F.; Juliano, C. *Farmaco* **1999**, *54*, 232. (b) Fricker, S. P. *Gold Bull.* **1996**, *29*, 53. (c) Elsome, A. M.; Hamilton-Miller, J. M. T.; Brumfitt, W.; Noble, W. C. *J. Antimicrob. Chemother.* **1996**, *37*, 911. (d) Berners-Price, S. J.; Johnson, R. K.; Giovenella, A. J.; Faucette, L. F.; Mirabelli, C. K.; Sadler, P. J. *J. Inorg. Biochem.* **1988**, *33*, 285. (e) Nomiya, K.; Noguchi, R.; Oda, M. *Inorg. Chim. Acta* **2000**, *298*, 24. (f) Nomiya, K.; Noguchi, R.; Shigeta, T.; Kondoh, Y.; Tsuda, K.; Ohsawa, K.; Kasuga, N. C.; Oda, M. *Bull. Chem. Soc. Jpn.* **2000**, *73*, 1143. (g) Nomiya, K.; Noguchi, R.; Ohsawa, K.; Tsuda, K.; Oda, M. *J. Inorg. Biochem.* **2000**, *78*, 363.

10.1021/ic990526o CCC: $19.00
Published on Web 06/28/2000

(I) interaction, whose energy is similar to that of hydrogen bonds, has been rationalized by using relativistic and correlation effects.[7] A second topic of interest is concerned with the helicity,[10] i.e., properties as helical polymers of d^{10} metals, most of which have been recently observed in the silver(I) complexes, e.g., several single-stranded helices such as $[Ag(1,2,3\text{-triz})(PPh_3)_2]_n$ (Htriz = triazole) and $[Ag(1,2,4\text{-triz})(PPh_3)_2]_n$[6c] and $[Ag(pydz)](NO_3)$ (pydz = pyridazine), $[Ag(pydz)](OTf)$ (OTf = CF_3SO_3), and $[Ag(pydz)_2](BF_4)$,[10a] a helix of [Ag(2,2′-biimidazole)](NO_3),[10e] and the double helix of [Ag(bpp)](OTf) (bpp = 1,3-bis(4-pyridyl)propane).[10d] Also, the helical polymer in the gold(I) complex has been elucidated for $Cs_2Na[Au_2(tma)(Htma)]$ (myocrisine; H_3tma = thiomalic acid) as showing antiarthritic action.[11]

In relation to bioinorganic silver(I) complexes, we have so far found that the two silver(I)−imidazole complexes, i.e., the noncrystalline, colorless powder of polymeric silver(I) imidazolate $[Ag(im)]_n$ (**4**; Him = imidazole) and monomeric crystalline complex $[Ag(Him)_2](NO_3)$ (**5**), have shown a wide spectrum of effective antibacterial and antifungal activities.[6a,b] Marked activities were also observed in other polymeric silver(I) complexes with various nitrogen-containing heterocyclic ligands such as $[Ag(1,2,3\text{-triz})]_n$,[6c] $[Ag(1,2,4\text{-triz})]_n$,[6c] $[Ag(pz)]_n$ (Hpz = pyrazole),[6d] and $[Ag(tetz)]_n$ (Htetz = tetrazole).[5e] Of particular note is the fact that it has been hard to design complexes that would show effective antifungal activities. The antimicrobial activities observed in the Ag^I−N bonding complexes were, in fact, in contrast to those of the Ag^I−S bonding complexes such as $\{Na[Ag(Htma)]\}_n$,[6e] $\{Na[Ag(mba)]\}_n$ (H_2mba = 2-mercaptobenzoic acid), and $[Ag(Hmba)]_n$,[6f,j] which have shown effective activities mostly against bacteria but not against fungi. The water-soluble salt $\{Na[Ag(mba)]\}_n$ has been commercialized as an antimicrobial agent.[6k]

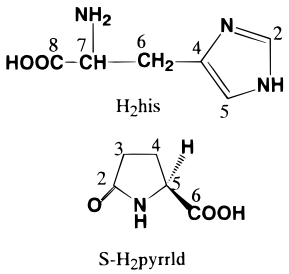

Figure 1. Abbreviation of ligands and their numbering for the NMR assignment.

However, in the practical viewpoint, there are serious problems, namely, that all polymeric Ag^I−N bonding complexes, including **4**, are water insoluble and the cationic, water-soluble Ag^I−N bonding complex **5** was light unstable. Thus, we have surveyed the silver(I) complexes that are water soluble and light stable, using 6 ligands with both nitrogen-containing heterocycle and carboxyl groups and also using 11 amino acids. In this work, we have successfully obtained the two desired silver(I) complexes, $\{[Ag(Hhis)]\cdot 0.2EtOH\}_2$ (**1**; H_2his = L-histidine) and $[Ag(Hpyrrld)]_2$ (**3**; $H_2pyrrld$ = (*S*)-(−)-2-pyrrolidone-5-carboxylic acid). The silver(I) histidinate complex was present as two different polymers in the solid state, i.e., the water-soluble powder **1** $\{[Ag(Hhis)]_2\}_n$ with the Ag−N bonding dimeric cores and the water-insoluble crystals formed by crystallization of **1**, i.e., $[Ag(Hhis)]_n$ (**2**) without a core complex. The X-ray crystal structures of **2** and **3** were determined.

Herein we report full details of the synthesis, characterization, and antibacterial and antifungal activities of **1**−**3**. The abbreviations of the ligands used here and the numbering for the NMR assignments of **1** and **3** are shown in Figure 1.

Experimental Section

Materials. The following were reagent grade used as received: L-histidine (H_2his), L-proline, L-tryptophan, (*S*)-(−)-2-pyrrolidone-5-carboxylic acid ($H_2pyrrld$), Ag_2O, $AgNO_3$, 1.0 M NaOH aqueous solution, glycine, L-alanine, L-serine, L-valine, L-lysine, L-(+)-glutamine, L-glutamic acid (all from Wako); imidazole-4,5-dicarboxylic acid (Tokyo Kasei); 1,2,3-triazole-4,5-dicarboxylic acid, pyrrole-2-carboxylic acid, urocanic acid, L-asparagine, DL-aspartic acid (Aldrich); D_2O (99.9 D atom %) (Isotec).

Instrumentation/Analytical Procedures. CHN elemental analyses were performed using Perkin-Elmer PE2400 series II CHNS/O analyzer. Thermogravimetric (TG) and differential thermal analysis (DTA) were carried out using a Rigaku TG 8101D and TAS 300 data processing system. TG/DTA measurements were run under air with a temperature ramp of 4 °C min^{-1} between 30 and 500 °C. Infrared spectra were recorded on a Jasco FT-IR 300 spectrometer in KBr disks at room temperature.

Molecular weight measurements in water based on the vapor pressure method were carried out by Mikroanalytishes Labor Pascher (Remagen, Germany) and evaluated for 15.89 mg of the complex **1** dissolved in 0.49529 g of water.

The ESI mass spectra were recorded using a TSQ 7000 mass spectrometer (Finnigan MAT) with an ESI source with an *m*/*z* range of 10−2000 with the resolution of unit mass at scan rate 2 s $scan^{-1}$. The data processing was performed with an ULTRIX on a DEC 3000 station (DEC). The electrospray interface was heated to 250 °C (or capillary temperature), the spray voltage was 4.5 kV, the sheath N_2 gas pressure was 70 psi, and a saturated aqueous solution of the sample was infused into the ESI source at flow rate of 3 μL min^{-1} using a 250-μL syringe and a syringe pump (Harvard Apparatus 22, Cambridge, MA).

(6) (a) Nomiya, K.; Tsuda, K.; Sudoh, T.; Oda, M. *J. Inorg. Biochem.* **1997**, *68*, 39. (b) Nomiya, K.; Tsuda, K.; Tanabe, Y.; Nagano, H. *J. Inorg. Biochem.* **1998**, *69*, 9. (c) Nomiya, K.; Tsuda, K.; Kasuga, N. C. *J. Chem. Soc., Dalton Trans.* **1998**, 1653. (d) Nomiya, K.; Noguchi, R.; Oda, M. Unpublished data. (e) Nomiya, K.; Onoue, K.; Kondoh, Y.; Kasuga, N. C.; Nagano, H.; Oda, M.; Sakuma, S. *Polyhedron* **1995**, *14*, 1359. The described $n = 15-19$ should be corrected to $n = 24-34$ as shown in: *Polyhedron* **1996**, *15*, 2303. (f) Nomiya, K.; Kondoh, Y.; Onoue, K.; Kasuga, N. C.; Nagano, H.; Oda, M.; Sudoh, T.; Sakuma, S. *J. Inorg. Biochem.* **1995**, *58*, 255. The described $n = 12-14$ should be corrected to $n = 21-27$. (g) Nomiya, K.; Kondoh, Y.; Nagano, H.; Oda, M. *J. Chem. Soc., Chem. Commun.* **1995**, 1679. (h) Nomiya, K.; Kasuga, N. C.; Takamori, I.; Tsuda, K. *Polyhedron* **1998**, *17*, 3519. (i) Nomiya, K.; Takahashi, S.; Noguchi, R. *J. Chem. Soc., Dalton Trans.* **2000**, 1343. (j) Nomiya, K.; Noguchi, R.; Kato, C. *Chem. Lett.* **2000**, 162. (k) Oda, M.; Itoh, H.; Sudo, T.; Sakuma, S.; Nomiya, K.; Suzuki, Y.; Jonoshita, Y.; Kikuchi, A.; Takabatake, Y. PCT, WO 95/12602, 1995.

(7) (a) Pyykko, P. *Chem. Rev.* **1997**, *97*, 597. (b) Pyykko, P.; Runeberg, N.; Mendizabal, F. *Chem. Eur. J.* **1997**, *3*, 1451. (c) Pyykko, P.; Mendizabal, F. *Chem. Eur. J.* **1997**, *3*, 1458. (d) Braga, D.; Grepioni, F.; Desiraju, G. R. *Chem. Rev.* **1998**, *98*, 1375. (e) Pathaneni, S. S.; Desiraju, G. R. *J. Chem. Soc., Dalton Trans.* **1993**, 319. (f) Zank, J.; Schier, A.; Schmidbaur, H. *J. Chem. Soc., Dalton Trans.* **1998**, 323. (g) Schmidbaur, H. *Chem. Soc. Rev.* **1995**, *24*, 391. (h) Angermaier, K.; Schmidbaur, H. *J. Chem. Soc., Dalton Trans.* **1995**, 559. (i) Hollatz, C.; Schier, A.; Riede, J.; Schmidbaur, H. *J. Chem. Soc., Dalton Trans.* **1999**, 111. (j) Harwell, D. E.; Mortimer, M. D.; Knobler, C. B.; Anet, F. A. L.; Hawthorne, M. F. *J. Am. Chem. Soc.* **1996**, *118*, 2679.

(8) (a) Jansen, M. *Angew. Chem., Int. Ed. Engl.* **1987**, *26*, 1098. (b) Dance, I. G. *Polyhedron* **1986**, *5*, 1037. (c) Dance, I. G.; Fitzpatrick, L. J.; Rae, A. D.; Scudder, M. L. *Inorg. Chem.* **1983**, *22*, 3785.

(9) See the examples of silver(I) complexes in Table 4 and references therein.

(10) (a) Carlucci, L.; Ciani, G.; Proserpio, D. M.; Sironi, A. *Inorg. Chem.* **1998**, *37*, 5941. (b) Wu, B.; Zhang, W.-J.; Yu, S.-Y.; Wu, X.-T. *J. Chem. Soc., Dalton Trans.* **1997**, 1795. (c) Psillakis, E.; Jeffery, J. C.; McCleverty, J. A.; Ward, M. D. *J. Chem. Soc., Dalton Trans.* **1997**, 1645. (d) Carlucci. L.; Ciani. G.; v. Gudenberg, D. W.; Proserpio, D. M. *Inorg. Chem.* **1997**, *36*, 3812. (e) Hester, C. A.; Baughman, R. G.; Collier, H. L. *Polyhedron* **1997**, *16*, 2893. (f) Suzuki, T.; Kotsuki, H.; Isobe, K.; Moriya, N.; Nakagawa, Y.; Ochi, M. *Inorg. Chem.* **1995**, *34*, 530.

(11) Bau, R. *J. Am. Chem. Soc.* **1998**, *120*, 9380.

^{1}H NMR (399.65 MHz) and ^{13}C{^{1}H} NMR (100.40 MHz) in solution were recorded at 25 °C in 5 mm outer diameter tubes on a JEOL JNM-EX 400 FT-NMR spectrometer with a JEOL EX-400 NMR data processing system. ^{1}H and ^{13}C{^{1}H} NMR spectra of the complexes were measured in D_2O solution with reference to an internal DSS. Chemical shifts are reported on the δ scale, and resonances downfield of DSS (δ 0) are recorded as positive. ^{109}Ag NMR (18.45 MHz) in solution were recorded at 25 °C in 10 mm outer diameter tubes on a JEOL JNM-EX 400 FT-NMR spectrometer equipped with a JEOL NM-40T10L low-frequency tunable probe. The ^{109}Ag NMR spectra of the complexes were measured in D_2O with reference to an external standard of saturated $AgNO_3-D_2O$ solution by a substitution method. Chemical shifts are reported on the δ scale with resonances downfield of $AgNO_3$ (δ 0) as positive. Spectral parameters for ^{109}Ag NMR include the following: pulse width 13.2 μs; acquisition time 0.39 s; recycle time 1.39 s; sweep width 21 008 Hz.

Solid-state ^{13}C NMR (67.94 MHz) and ^{15}N NMR (27.38 MHz) spectra were measured using a JEOL EX 270 WB spectrometer equipped with a cross-polarization (CP)/magic angle spinning (MAS) accessory. The ^{13}C and ^{15}N NMR spectral widths were 27.0 and 42.0 kHz, respectively. Data points of ^{13}C and ^{15}N NMR spectra were 8 k. A silicon nitride ceramic cylindrical-type rotor was used. The spinning rate was set to about 5.5 kHz. Usually,^{13}C and ^{15}N spectra were accumulated 1200−1500 and 10 000−12 000 times at a repetition time of 5 s to achieve a reasonable signal-to-noise ratio, respectively. A variable-temperature (VT) controller was used for all of the probe temperatures at which measurements were taken. The VT-^{13}C CP/MAS NMR spectra were also measured over the temperature range 25 to 140 °C. The ^{13}C and ^{15}N NMR chemical shifts were calibrated indirectly through external hexamethylbenzene [17.3 ppm relative to TMS (δ 0)] and directly external NH_4NO_3 (NH_4: δ 0), respectively. In the ^{13}C NMR measurements, the quaternary carbons were assigned by the MASDL (magic angle spinning dipolar dephasing) method, i.e., the CP/MAS method with dipolar dephasing. The experimental errors of the isotropic ^{13}C and ^{15}N NMR chemical shift values were estimated to be about 0.5 ppm. Spinning sidebands scarcely appeared due to the sufficient spinning rate.

Preparations. {[Ag(Hhis)]·0.2EtOH}$_2$ (1) as a Water-Soluble Powder. To a suspension of 0.232 g (1.0 mmol) of Ag_2O in 10 mL of water was added a solution of 0.620 g (4.0 mmol) of H_2his in 20 mL of water. During 2 h of stirring, the black suspension changed to a clear yellow solution. [Note: longer stirring, e.g., 12 h or more, gave a water-insoluble white powder with the same composition as **1**, the IR spectrum of which was different from that of **1**.] Unreacted black powder of Ag_2O was filtered off through a folded filter paper (Whatman No. 5). The clear yellow filtrate was added dropwise to 250 mL of ethanol. The white powder formed was collected on a membrane filter (JG 0.2 μm), washed with ether (100 mL × 2), and dried in vacuo. The light-stable and thermally stable white powder obtained in 0.39 g (72.1%) yield was soluble in water but insoluble in most organic solvents. Solubility in water at room temperature was 5.66 mg mL^{-1}. The synthetic procedure was successfully scaled-up by a factor of 10, resulting in a 4.78 g (88.1%) yield. Anal. Found: C, 28.15; H, 3.63; N, 15.82. Calcd for $C_{6.4}H_{9.2}N_3O_{2.2}Ag$ or [Ag(Hhis)]·0.2EtOH as a monomer unit: C, 28.34; H, 3.42; N, 15.49. TG/DTA data: 3.19% weight loss was observed before decomposition temperature; calcd 3.39% for $x = 0.2$ in [Ag(Hhis)]·xEtOH. Decomposition began around 196 °C with endothermic peaks at 91 and 255 °C and an exothermic peak at 197 °C. Solution molecular weight measurement: 442 in water; calcd 524.0 for $[Ag(Hhis)]_2$. Measurements of the MALDI mass spectra were unsuccessful. A positive-ion ESI mass, a molecular ion peak, $[M + H]^+ = m/z$ 525.0, was observed for M = $[Ag(Hhis)]_2$. Prominent IR bands in the 1700−400 cm^{-1} region (KBr disk): 1635 vs, 1577 s, 1459 vs, 1417 s, 1342 m, 1314 m, 1271 m, 1252 m, 1148 m, 977 m, 967 m, 925 m, 837 m, 777 m, 624 m, 537 w, 426 w cm^{-1}. ^{1}H NMR (D_2O, 25 °C): δ 1.17 (EtOH), 3.65 (EtOH), 3.06−3.24 (H6, two double doublets, 2H), 3.75−3.79 (H7, doublet of doublet, 1H), 7.12 (H5, s, 1H), 7.81 (H2, s, 1H) ppm. ^{13}C NMR (D_2O, 25 °C): δ 19.5 (EtOH), 60.1 (EtOH), 35.3 (C6), 59.6 (C7), 119.8 (C5), 136.4 (C4), 140.4 (C2), 181.0 (C8) ppm. ^{109}Ag NMR (D_2O, 25 °C): δ 476 ppm. Solid-state ^{13}C NMR (24.1 °C): δ 33.2 (C6), 57.2 (C7), 116.1 (C5), 127.8 (C2), 137.5 (C4), 179.0 (C8) ppm. Solid-state ^{15}N NMR (24.5 °C, BF = 200 Hz, referenced to NH_4NO_3): δ −40.5 (N_{amino}), 112.4 (N_τ), 149.5 (N_π) ppm.

Solution ^{13}C NMR of H_2his ligand (D_2O, 25.6 °C): δ 31.0 (C6), 57.6 (C7), 119.5 (C5), 135.0 (C4), 139.1 (C2), 176.8 (C8) ppm. Solid-state ^{13}C NMR of H_2his ligand (24.0 °C): δ 27.2 (C6), 57.5 (C7), 114.2 (C5), 135.1 (C2), 137.6 (C4), 175.3 (C8) ppm. Solid-state ^{15}N NMR of H_2his ligand (25.0 °C, BF = 10 Hz, referenced to NH_4NO_3): δ 19.2 (N_{amino}), 148.9 (N_τ), 227.3 (N_π) ppm.

In the pH measurements of saturated aqueous solution of **1**, the solution became cloudy, probably because of dissociation of the silver(I) ion in the presence of the Cl^- ion and the resulting precipitation of AgCl. When $AgNO_3$ as the starting material was used, instead of Ag_2O, the final product was contaminated with the NO_3^- ion which was hard to remove. The reaction with Ag_2O:H_2his:NaOH = 1:4:2 molar ratio also gave the product with the same IR and ^{1}H NMR spectra as **1** obtained under the conditions without NaOH. However, the 1:4:4 and 1:4:8 ratio reactions gave clear gel materials different from the solid **1**.

[Ag(Hhis)]$_n$ (2) as Water-Insoluble Crystals. Crystallization of **1** was carried out by slow evaporation from an aqueous solution and/or vapor diffusion of an internal aqueous solution of **1** with an external solvent, acetone, both of which gave water-insoluble, colorless plate crystals. During a few days of standing at room temperature, crystals suitable for single-crystal X-ray diffraction studies were grown. The CHN analysis of the water-insoluble crystals showed that their composition consisted of Ag:Hhis$^-$ = 1:1, but the IR and solid-state ^{13}C and ^{15}N NMR spectra were significantly different from those of **1**. The crystals obtained by slow evaporation were characterized as below. Anal. Found: C, 27.78; H, 2.76; N, 15.74. Calcd for $C_6H_8N_3O_2Ag$ or [Ag(Hhis)] as a monomer unit: C, 27.50; H, 3.08; N, 16.04. TG/DTA data: no weight loss was observed before decomposition temperature. Decomposition began around 183 °C with exothermic peaks at 213, 240, and 403 °C. Prominent IR bands in the 1700−400 cm^{-1} region (KBr disk): 1632 m, 1575 vs, 1462 m, 1402 s, 1343 m, 1255 w, 1148 w, 973 w, 912 w, 835 m, 780 m, 624 m, 551w cm^{-1}. Solid-state ^{13}C NMR (24.8 °C): δ 38.3 (C6), 57.9 (C7), 114.1 (C5), 137.4 (C4), 140.7 (C2), 180.6 (C8) ppm. Solid-state ^{15}N NMR (24.7 °C, BF = 200 Hz, referenced to NH_4NO_3): δ 1.1 (N_{amino}), 159.4 (N_τ), 191.3 (N_π) ppm.

[Ag(Hpyrrld)]$_2$ (3). To a suspension of 0.232 g (1.0 mmol) of Ag_2O in 10 mL of water was added a solution of 0.258 g (2.0 mmol) of H_2pyrrld in 10 mL of water. During 2 h of stirring, the black suspension gradually changed to a clear orange solution. Unreacted black powder of Ag_2O was filtered off through a folded filter paper (Whatman No. 5). The clear colorless filtrate was added dropwise to 50 mL of acetone. The white powder formed was collected on a membrane filter (JG 0.2 μm), washed with ether (50 mL × 2), and dried in vacuo. The light-stable, milk-white powder obtained in 0.36 g (76.0%) yield was soluble in water, sparingly soluble in DMSO, but insoluble in most organic solvents. Solubility in water at room temperature was 13.64 mg mL^{-1}. By the heating of the aqueous solution, this complex decomposed to form undissolved brown flakes. The synthetic procedure was successfully scaled-up by a factor of 5, resulting in 1.15 g (48.7%) yield. Anal. Found: C, 25.10; H, 2.27; N, 5.79. Calcd for $C_5H_6NO_3Ag$ or [Ag(Hpyrrld)] as a monomer unit: C, 25.45; H, 2.56; N, 5.94. TG/DTA data: no weight loss was observed before decomposition temperature. Decomposition began around 188 °C with an exothermic peak at 194 °C. Solution molecular weight measurement failed; there were undissolved brown flakes after the sample was warmed for dissolution. Measurements of the MALDI mass spectra were unsuccessful. A positive-ion ESI mass, a molecular ion peak, $[M + H]^+ = m/z$ 472.9, was observed for M = $[Ag(Hpyrrld)]_2$. Prominent IR bands in the 1700−400 cm^{-1} region (KBr disk): 1676 vs, 1593 vs, 1458 w, 1407 s, 1298 s, 1154 w, 1106 w, 1042 w, 1010 w, 721 m, 496 m cm^{-1}. ^{1}H NMR (D_2O, 25 °C): δ 1.98−2.07 (H4a, m, 1H), 2.37−2.41 (H3, m, 2H), 2.45−2.55 (H4b, m, 1H), 4.16−4.19 (H5, double doublet, 1H) ppm. ^{13}C NMR (D_2O, 25 °C): δ 28.1 (C4), 32.4 (C3), 61.0 (C5), 183.0 (C6), 184.5 (C2) ppm. Solid-state ^{13}C NMR (24.4 °C): δ 26.2 (C4), (29.8, 32.9) (C3), 59.3 (C5), (177.6, 179.9) (C6), (181.6, 182.3) (C2) ppm. Solid-state ^{15}N NMR (24.0 °C, BF = 120 Hz, referenced to NH_4NO_3): δ 72.3 ppm.

Table 1. Summary of Crystal Data for the Complexes **2** and **3**

	2	**3**
semiempirical formula	$C_6H_8N_3O_2Ag$	$C_{10}H_{12}N_2O_6Ag_2$
fw	262.02	471.95
T, K	296	296
cryst system	monoclinic	monoclinic
space group	$P2_1$ (No. 4)	$P2_1$ (No. 4)
a (Å)	5.739(1)	5.2051(8)
b (Å)	7.671(2)	12.736(2)
c (Å)	9.040(1)	9.773(1)
β (deg)	104.73(1)	95.162(6)
V (Å^3)	384.9(1)	645.2(1)
Z	2	2
λ, Å (Mo Kα)	0.710 69	0.710 69
μ, cm^{-1}	25.69	30.53
goodness-of-fit index	1.29	1.09
no. of unique reflcns	959	1352
no. of obsd reflcns ($I > 2.0\sigma(I)$)	834	1266
R_F[a]	0.024	0.026
R_{wF}[b]	0.028	0.030

[a] $R_F = \sum[|F_o| - |F_c|]/\sum|Fo|$. [b] $R_{wF} = [\{\sum w(|F_o| - |F_c|)^2\}/\{\sum w(|F_o|)^2\}]^{1/2}$.

Crystallization of **3** was carried out by vapor diffusion of an internal aqueous solution of **3** with an external solvent, acetone, which gave water-soluble colorless needle crystals. The crystals of sufficient quality suitable for single-crystal X-ray diffraction studies were grown by the second vapor diffusion using the first isolated crystals. The CHN analysis and FT-IR measurements showed that the single crystals were representative of the bulk materials of **3**. In the pH measurements of saturated aqueous solution of **3**, the solution became cloudy, probably because of dissociation of the silver(I) ion under the Cl^- ion and the precipitation of AgCl.

In the synthetic procedure with a minor modification, $AgNO_3$ can be used, instead of Ag_2O, and the same product was obtained without NO_3^- contamination. To a solution of 0.169 g (1.0 mmol) of $AgNO_3$ in 10 mL of water was added a solution of 0.129 g (1.0 mmol) of H_2pyrrld in 10 mL of water. The colorless solution was stirred for 1 h. To it, 1.0 mL of 1.0 M NaOH aqueous solution (1.0 mmol) was added dropwise and the stirring was continued for 2 h. The clear colorless solution was added dropwise to 50 mL of acetone. The white precipitate formed was collected on a membrane filter (JG 0.2 μm), washed with ether (50 mL × 2), and dried in vacuo. A light-stable milk-white powder was obtained in 0.20 g (86.0%) yield.

X-ray Crystallography. Single crystal of **2** was mounted on glass fiber and transferred to a Rigaku AFC5S diffractometer, and the intensity date were collected at 296 K. The data were corrected for Lorentz and polarization effects, and empirical absorption corrections based on PSI scans were applied to the data of **2**. The overall averaged transmission factor of **2** was in the range of 0.724−0.999. The intensity data of **3** were collected at 296 K on a Rigaku R-AXIS RAPID imaging-plate diffractometer. A self-consistent semiempirical absorption correction based on Fourier coefficient fitting of symmetry-equivalent reflections was applied using the ABSCOR program.[12b]

The structures were solved by direct methods followed by subsequent difference Fourier calculation and refined by a full-matrix least-squares procedure using the TEXSAN package.[12a] All non-hydrogen atoms were refined anisotropically and hydrogen atoms isotropically. Crystal data, data collection, and structure refinement of **2** and **3** are summarized in Table 1.

Antibacterial and Antifungal Activities. Antimicrobial activities of silver(I) complexes were estimated by minimum inhibitory concentration (MIC: μg mL^{-1}) as usual.[6a,c,e,f,k] Bacteria and yeast were inoculated into 5 mL of liquid medium (soybean casein digest (SCD) medium for bacteria and glucose peptone (GP) medium for yeast) and cultured for 24 h at 35 °C and 48 h at 30 °C, respectively. The cultured fluids were adjusted to the cell concentration of 10^6-10^7 mL^{-1} and used for inoculation in the MIC test. As for the mold culture, the agar slant (potato dextrose (PD) agar medium) for 1 week cultivation at 27 °C was washed with saline containing 0.05% Tween 80. The spore suspension obtained was adjusted to the concentration of 10^6 mL^{-1} and used for inoculation in the MIC test.

The test materials **1**−**3** and free ligands, H_2his and H_2pyrrld, were added to each culture medium and then diluted two times with each culture medium. A 1 mL volume of each of the culture mediums containing various concentrations of test materials was inoculated with 0.1 mL of the microorganism suspension prepared above.

Bacteria were cultured for 24 h at 35 °C, yeast for 48 h at 30 °C, and mold for 1 week at 25 °C, and then the growth of microorganisms was observed. When no growth of microorganisms was observed in the medium containing the lowest concentration of test materials, the MIC of the test material was defined at this point of dilution.

SCD, GP, and PD media were purchased from Nissui.

Results and Discussion

Survey Experiments. Test ligands used here were 6 ligands with both nitrogen-containing heterocycle and carboxyl groups; L-proline, pyrrole-2-carboxylic acid, urocanic acid, 1,2,3-triazole-4,5-dicarboxylic acid, imidazole-4,5-dicarboxylic acid, and (*S*)-(−)-2-pyrrolidone-5-carboxylic acid (H_2pyrrld), and also 11 amino acids, glycine, L-alanine, L-serine, L-valine, L-asparagine, DL-aspartic acid, L-lysine, L-(+)-glutamine, L-glutamic acid, L-tryptophan, and L-histidine (H_2his). To a solution or a suspension of the test ligand (0.5, 1.0, and 2.0 mmol) in 1.0 mL of water was added 1.0 mL of 1 M $AgNO_3$ aqueous solution, followed by adding 1.0 mL of 1 M NaOH aqueous solution. It was qualitatively examined whether the water-soluble and light-stable compounds were formed. The ligands, which gave black precipitates by adding NaOH aqueous solution and/or did not form a colorless solid from the colorless clear aqueous solution by reprecipitation with excess amounts of ethanol or acetone, were excluded as a candidate. Finally, H_2his and H_2pyrrld ligands were selected, and isolation of their pure silver(I) complexes was carried out (see the Experimental Section).

If the addition of 1.0 mL of 1 M NaOH aqueous solution is skipped in this workup, we can see many possible silver(I) complexes with the ligands used for the tests. As a matter of fact, X-ray crystal structures of silver(I)−glycinate complexes $[Ag(gly)]_n$[13a] and $\{[Ag(gly)]\cdot 0.5H_2O\}_n$,[13a] silver(I)−α-alaninate, $[Ag(\alpha\text{-ala})]_n$,[13b] and silver(I)−$\beta$-alaninate nitrate, $[Ag_2(\beta\text{-ala})_2](NO_3)_2$,[13c,d] have been so far reported. However, these complexes are stable only in the solid state.

Compositional Characterization. The compositions of **1** and **3**, written as $\{[Ag(Hhis)]\cdot 0.2EtOH\}_2$ and $[Ag(Hpyrrld)]_2$, respectively, were consistent with all data for elemental analysis, TG/DTA, FT-IR, and ^{1}H and ^{13}C NMR spectra. In **1**, the presence of 0.2 equiv of EtOH solvate was confirmed from elemental analysis data, weight loss observed in TG/DTA measurements, and ^{1}H and ^{13}C NMR spectra. On the other hand, **3** was isolated without any solvated molecules. In the ESI mass spectrometry, molecular ion peaks of **1** and **3** were detected. Solution molecular weight measurements of **1** suggested that this complex was possibly present as a dimer in aqueous solution.

On the other hand, the X-ray crystallography revealed that **3** in the solid state was a helical polymer formed by weak

(12) (a) TEXSAN: Crystal Structure Analysis Package, Molecular Structure Corp., Houston, TX, 1985 and 1992. (b) Higashi, T. ABSCOR: Program for Absorption Correction, Rigaku Corp., Tokyo, Japan, 1995.

(13) (a) Acland, C. B.; Freeman, H. C. *J. Chem. Soc., Chem. Commun.* **1971**, 1016. (b) Demaret, P. A.; Abraham, F. *Acta Crystallogr.* **1987**, *C43*, 1519. (c) Kamwaya, M. E.; Papavinasam, E.; Teoh, S. G.; Rajaram, R. K. *Acta Crystallogr.* **1984**, *C40*, 1318. (d) Kamwaya, M. E.; Papavinasam, E.; Teoh, S. G.; Rajaram, R. K. *Z. Kristallogr.* **1984**, *169*, 51.

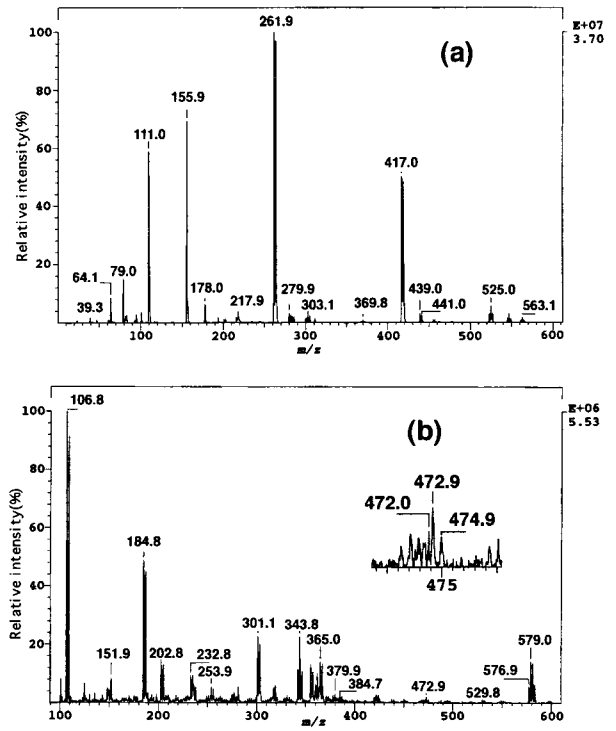

Figure 2. Positive-ion ESI mass spectra measured in aqueous solution of (a) **1** in the range *m*/*z* 20−600 and of (b) **3** in the range *m*/*z* 100−600. In (b), the inset shows an enlargement around the peak *m*/*z* 472.9.

Table 2. Selected Bond Distances (Å) and Angles (deg) for the Complexes **2** and **3**

2		**3**	
Ag1−N3^{ii}	2.097(4)	Ag1−Ag1(a)	2.9022(7)
Ag1−N9	2.125(4)	Ag1−O1	2.188(5)
		Ag1−O2(a)	2.217(5)
		Ag1(a)−O2	2.220(4)
		Ag1(a)−O1(a)	2.186(5)
		O1−C6	1.226(8)
		O2−C6	1.248(7)
		O3−C2	1.239(8)
		O1(a)−C6(a)	1.252(8)
		O2(a)−C6(a)	1.251(8)
		O3(a)−C2(a)	1.245(8)
		N1−C2	1.340(8)
		N1−C5	1.455(8)
		N1(a)−C2(a)	1.318(9)
		N1(a)−C5(a)	1.464(8)
		Ag1^{i}−O3	2.470(4)
N3^{ii}−Ag1−N9	166.8(2)	O1−Ag1−O2(a)	158.7(2)
Ag1^{i}−N3−C2	130.0(4)	O1(a)−Ag1(a)−O2	163.6(2)
Ag1^{i}−N3−C4	123.4(3)	Ag1−Ag1(a)−O2	79.2(1)
Ag1−N9−C7	121.5(3)	Ag1(a)−Ag1−O2(a)	78.0(1)
		Ag1−Ag1(a)−O1(a)	84.5(1)
		Ag1(a)−Ag1−O1	82.3(1)
		Ag1−O1−C6	124.1(4)
		Ag1(a)−O1(a)−C6(a)	122.0(4)
		Ag1−O2(a)−C6(a)	128.9(4)
		Ag1(a)−O2−C6	126.1(4)
		O1−C6−O2	126.8(6)
		O1(a)−C6(a)−O2(a)	126.4(6)

interactions between the dimeric core, while **2** was a helical polymer without a core complex. Solid-state ^{15}N and ^{13}C NMR spectroscopies showed the polymeric nature of **1** in the solid state. Thus, **1**−**3** in the solid state can be represented as $\{[Ag(Hhis)]_2\}_n$, $[Ag(Hhis)]_n$, and $\{[Ag(Hpyrrld)]_2\}_n$, respectively.

The solid-state FT-IR spectra showed that the carbonyl stretching bands of the coordinating Hhis$^-$ ligand in **1** appeared at 1635 and 1577 cm^{-1} and that in **2** appeared at 1632 and 1575 cm^{-1}, while those of the free H_2his ligand appeared at 1636 and 1587 cm^{-1}. The bands in these regions suggest the existence of a deprotonated carboxyl group in the two complexes and the free ligand. The almost unchanged carbonyl stretching bands reflect the properties as zwitterion of this amino acid, suggesting no coordination of the carboxyl oxygen donor atoms to the silver(I) center. Thus, in **1** and **2** the coordination to the silver(I) atom is accomplished with the nitrogen donor atoms of the monoanionic Hhis$^-$ ligand. This bonding mode is supported by the solid-state ^{15}N NMR and also is consistent with the results of X-ray analysis of **2**.

On the other hand, the solid-state FT-IR spectrum of **3** showed that multiple vibrational bands in the region 3100−2600 cm^{-1} observed in the free H_2pyrrld ligand disappeared, and one very intense vibrational band around 3400 cm^{-1} appeared after complexation. The carbonyl stretching bands of the free ligand at 1720 and 1648 cm^{-1} were shifted to 1676 and 1593 cm^{-1} after the complexation. These facts also suggest that the peptide bond of −C(O)−NH− in the ring is potentially maintained in **3**, i.e., the keto form of the ligand participates in the coordination (Figure 1), and the two carboxyl oxygen atoms accomplish the formation of the dimeric silver(I) unit. This feature is also consistent with the results of X-ray crystallography.

ESI Mass Spectra. In mass spectrometry of silver-containing compounds, the presence of the two isotopes ^{107}Ag (51.8392%) and ^{109}Ag (48.1608%) is especially useful, particularly for cluster compounds composed of several silver atoms, because their mass spectra should give doublet peaks with almost equal intensity for a monometallic species and triplets with about 1:2:1 intensity ratio for a bimetallic species, and their isotopic distribution can then be utilized for identification of such compounds.[6g] In this work, we have successfully obtained the positive-ion ESI mass spectra of the bimetallic species using aqueous solutions of **1** and **3**, although the measurements of their matrix-assisted-laser-desorption ionization (MALDI) mass spectra were unsuccessful.

The positive-ion ESI mass spectra of **1** in the range of *m*/*z* 20−600 (Figure 2a) showed a three-line peak with an almost 1:2:1 intensity ratio indicative of a bimetallic species $\{H[Ag(Hhis)]_2\}^+$ (*m*/*z* 525.0, calcd *m*/*z* 525.0) and its fragmentation peaks based on protonation and/or elimination of the silver(I) and Hhis$^-$ ions accounting for the observed two two-line peaks with almost equal intensity indicative of the monometallic species $\{H_2[Ag(Hhis)_2]\}^+$ (*m*/*z* 417.0, calcd *m*/*z* 418.1) and $\{H[Ag(Hhis)]\}^+$ (*m*/*z* 261.9, calcd *m*/*z* 263.0) and of free ligand $\{H(H_2his)\}^+$ (*m*/*z* 155.9, calcd *m*/*z* 156.0). Calculated isotopic distributions of each fragment were in good agreement with the observed spectra. Thus, the peak $[M + H^+]^+$ (*m*/*z* 525.0), where M = $[Ag(Hhis)]_2$, is due to a molecular ion of **1**, suggesting its dimeric structure.

The positive-ion ESI mass spectra of **3** in the range of *m*/*z* 100−600 (Figure 2b) showed triplet peaks with an almost 1:2:1 intensity ratio indicative of bimetallic species $\{H[Ag(Hpyrrld)]_2\}^+$ (*m*/*z* 472.9, calcd *m*/*z* 472.9) and $\{[Ag_2(Hpyrrld)]\}^+$ (*m*/*z* 343.8, calcd *m*/*z* 343.8); the latter is a fragmentation based on elimination of H_2pyrrld from the former. It should be noted that a quartet peak with an almost 1:3:3:1 ratio assignable to $\{[Ag_3(Hpyrrld)_2]\}^+$ (*m*/*z* 579.0, calcd *m*/*z* 579.8) appears as a relatively larger peak. However, this peak is due to fragmentation based on deprotonation and attachment of the silver(I) ion among a bimetallic species in the helical polymer but not fragmentation from the discrete trimetallic molecular ion. In fact, since single-crystal X-ray analysis of **3** in the solid state revealed its dimeric structure as a constituent fundamental unit,

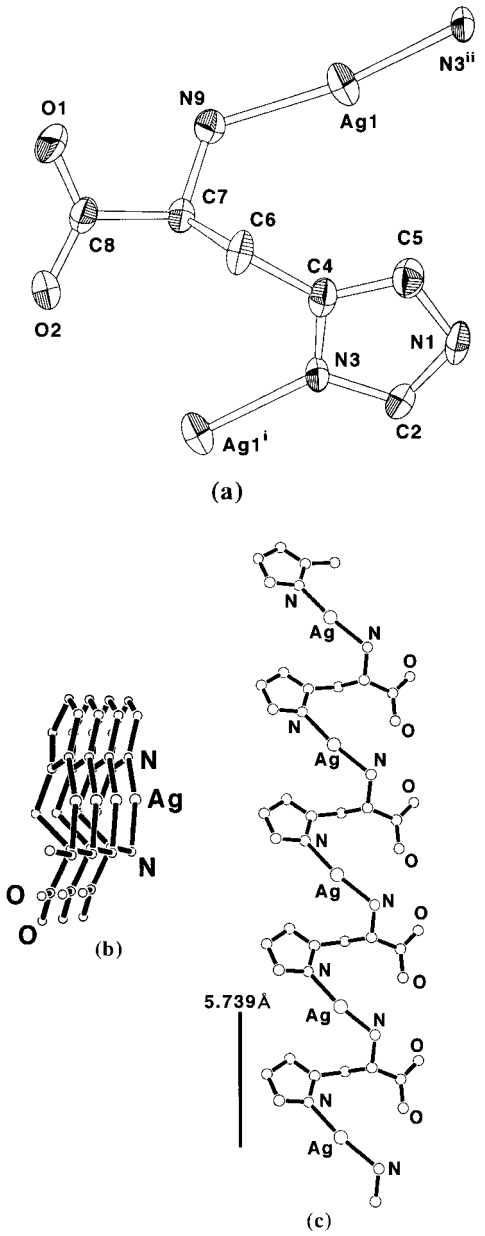

Figure 3. (a) Molecular structure of the local coordination around silver(I) centers of **2** with 50% probability ellipsoids (symmetry operation: i, $x - 1$, y, z; ii, $x + 1$, y, z), (b) top view of the main axis showing approximate 2-fold helical symmetry of the structure, and (c) side view of the left-handed helical polymer chain extended along the crystallographic *a* axis with a pitch 5.739 Å.

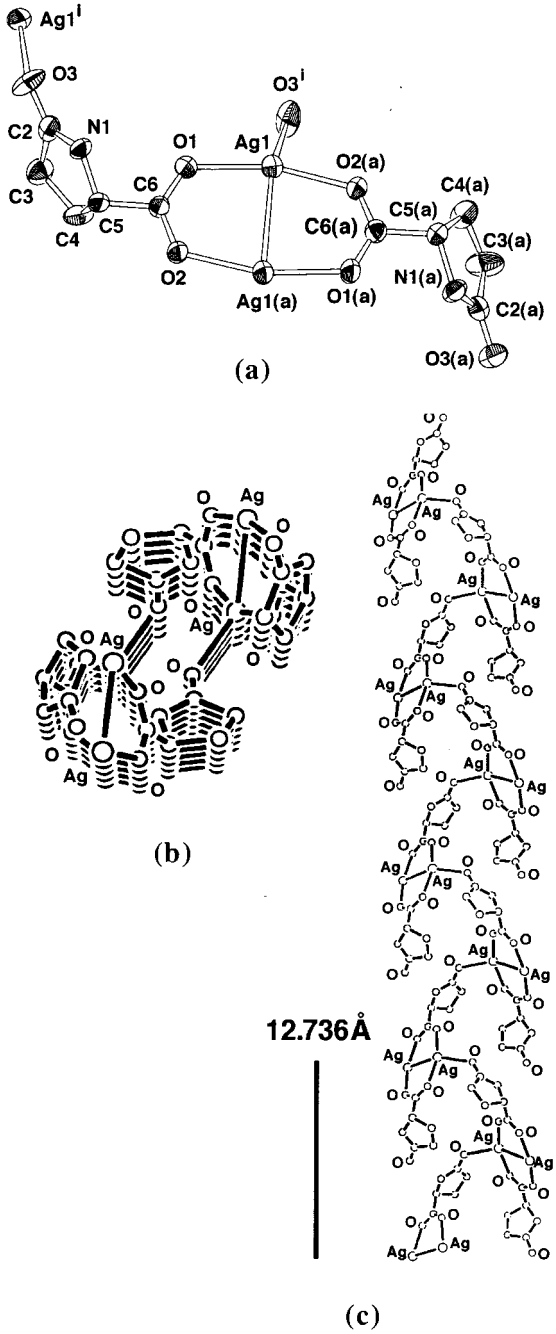

Figure 4. (a) Molecular structure of the local coordination around silver(I) centers of **3** with 50% probability ellipsoids (symmetry operation: i, $-x + 3$, $y - 0.5$, $-z + 2$), (b) top view of the main axis showing approximate 2-fold helical symmetry of the structure, and (c) side view of the left-handed helical polymer chain extended along the crystallographic *b* axis with a pitch 12.736 Å.

the molecular ion of the fundamental unit of **3** is a bimetallic species and not a trimetallic species. Thus, the peak $[M + H^+]^+$ (*m*/*z* 472.9), where M = $[Ag(Hpyrrld)]_2$, is assignable to a molecular ion of the fundamental unit of **3**. The calculated isotopic distributions of each fragment were also in good agreement with the observed spectra.

Crystal and Molecular Structures of 2 and 3. The molecular structures of **2** and **3** with the atom numbering scheme are depicted in Figures 3a and 4a, respectively. Selected bond distances and angles with their estimated standard deviations are listed in Table 2.

As shown in Figure 3a, the crystal structure of **2** is a polymer consisting of a bent, 2-coordinate silver(I) atom linking with the N_{amino} atom (N9) in one $Hhis^-$ ligand and the imidazole N_π atom (N3) in a different $Hhis^-$ ligand, in which the imidazole N_τ atom (N1) and carboxyl oxygen atoms do not participate in the coordination to the silver(I) center. This bonding mode is also consistent with the solid-state ^{15}N NMR measurements. The crystal structure consists of the packing of left-handed 2-fold single helices running along the crystallographic *a* axis, with a pitch of 5.739 Å (Figures 3b,c). This chiral polymer is formed with the chiral L-form of $Hhis^-$. In the molecular structure of **2**, the bent AgN_2 moiety contains the distances of Ag1−N9 (2.125(4) Å) and Ag1−N3^{ii} (2.097(4) Å), and the angle N3^{ii}−Ag1−N9 166.8(2)°. The bonding mode of **2** is unique because $O_{carboxyl}$ atoms do not participate in the coordination, and therefore, it is quite different from those of the known silver-

Table 3. Comparison of Silver(I) and Gold(I) Complexes with Helical Polymer Structures[a]

complexes	screw axis	pitch of the helix (Å)	ref
[Ag(pydz)](NO_3)	2_1	3.68	10a
[Ag(pydz)](CF_3SO_3)	2_1	5.40	10a
[Ag(pydz)$_2$](BF_4)	4_1	11.166	10a
[Ag(*R*,*R*-DIOP)(NO_3)]$_n$[b]	2_1	16.186	10b
{[Ag(*R*,*R*−L)](OTf)}$_n$[b]	2_1	*d*	10f
[Ag(2,2′-biimidazole)](NO_3)	3_1	*d*	10e
[Ag(2,4′-bipy)]X (X = NO_3^-, ClO_4^-)	*d*	*d*	18d
[Ag(bpp)](OTf)	double helix	21.1	10d
[Ag(1,2,3-triz)(PPh_3)$_2$]$_n$	2_1	9.12	6c
[Ag(1,2,4-triz)(PPh_3)$_2$]$_n$	2_1	9.53	6c
[Ag(tetz)(PPh_3)$_2$]$_n$	2_1	9.471	5e
[Ag(Hhis)]$_n$[b] (**2**)	2_1	5.739	*c*
[Ag(Hpyrrld)]$_2$[b] (**3**)	2_1	12.736	*c*
[Ag(*S*-othf)]$_2$[b]	2_1	5.416	6i
$Cs_2Na[Au_2(tma)(Htma)]$	double helix	*d*	11

[a] (*R*,*R*)-DIOP = (4*R*,5*R*)-*trans*-4,5-bis[(diphenylphosphino)methyl]-2,2-dimethyl-1,3-dioxalane; *R*,*R*−L = (4*R*,5*R*)-4,5-bis(2-(2-pyridyl-)ethyl)-1,3-dioxolane. [b] Chiral helical polymer. [c] This work. [d] Not described.

(I)−amino acid complexes, e.g., [Ag(gly)]$_n$[13a] and [Ag(α-ala)]$_n$[13b] as polymers of 2-coordinate linear O−Ag(I)−N cores (O−Ag−N angle 177 and 180(8)°, respectively), {[Ag(gly)]·0.5H_2O}$_n$, in which alternate silver(I) ions are bound to two $O_{carboxyl}$ and two N_{amino} atoms, respectively,[13a] and {[Ag(Hglygly)](NO_3)}$_2$ (Hglygly = glycylglycine)[13a] and {[Ag(*β*-ala)](NO_3)}$_2$[13c,d] as bis(carboxylato)-bridged dimers, in which the N_{amino} atoms do not participate in the coordination.

As illustrated in Figure 4b,c, the crystal structure of **3** is an unusual single-stranded helical polymer, a 2_1 helix, which is composed of noncentrosymmetric, bis(carboxylato-*O*,*O*′)-bridged [Ag(Hpyrrld)]$_2$ dimeric units, with the carboxylato group acting in the syn−syn bridging mode. This polymer has been unexpectedly obtained from self-assembly of the dimeric units. The crystal structure consists of the packing of left-handed 2-fold single helices, with a period along the crystallographic *b* axis, i.e., a pitch of 12.736 Å. The helicity of **3** in the solid state was accomplished with a connection of the ring carbonyl oxygen atom (O3) of one dimeric unit to one of the silver(I) centers of the adjacent dimeric unit. This chiral polymer is constructed with the chiral ligand, i.e., the *S*-form of $Hpyrrld^-$.

The helical polymer of **3** is compared with several examples of an infinite helical species listed in Table 3. In particular, the chiral helicity of **3** can be also compared with the recent, chiral helical polymers formed by self-assembly of the dimeric [Ag(othf)]$_2$ cores (*S*- and *R*-Hothf = (*S*)-(+)- and (*R*)-(−)-5-oxo-2-tetrahydrofurancarboxylic acid, respectively) and their racemic form as a stairlike polymer, {[Ag$_2$(*S*-othf)(*R*-othf)]}$_n$, all showing wide spectra of remarkably effective antibacterial and antifungal activities.[6i]

In the molecular structure of **3**, the keto form of the ligand coordinates to the silver(I) center, because the peptide bonding mode of −C2(O3)−N(1)H− is maintained. The O3 atom coordinates to a different silver atom, Ag1^i, and the Ag1 atom coordinates to a different oxygen atom, O3^i. The bonding between the dimeric units via O3 and O3^i atoms is weak (O3−Ag1^i distance 2.470(4) Å). The silver(I)−silver(I) separation (2.9022(7) Å) observed in the dimeric unit is close to that of metallic silver (2.88 Å)[14a] and significantly less than twice the van der Waals radii for silver (3.44 Å),[14b] indicating the presence of an intramolecular metal−metal interaction.[15] In comparison, the silver(I)−silver(I) distances and coordination numbers of the silver(I) atoms excluding and including the silver(I)−silver(I) bonds in several examples of the recent silver(I) clusters are listed in Table 4. The silver(I)−silver(I) distance of **3** is comparable to those found in the dimeric structures of known silver(I) carboxylates listed in Table 4 (entries 5−11). In Table 4, the silver(I)−silver(I) distances are found to be significantly influenced by the softness of the coordinating donor atoms. The shortest are within the Ag−O bonding clusters, and the more enhanced softness of the donor atoms gives rise to the longer silver(I)−silver(I) distances.

In **3**, two silver(I) centers, as well as two coordinated $Hpyrrld^-$ ligands, within the dimeric unit were unequivalent, i.e., they are 3-coordinate and 2-coordinate silver(I) atoms if the Ag−Ag interaction is not taken into account. Thus, the dimeric units are noncentrosymmetric. The molecular structure of the fundamental unit of **3** is compared with those of the two centrosymmetric silver(I) carboxylate complexes of triethyl betaine ($Et_3N^+CH_2CO_2^-$; Et_3Bet),[16a] i.e., [Ag$_2$(Et_3Bet)$_2$(NO_3)$_2$] and [Ag$_2$(Et_3Bet)$_2$]$_n$(ClO_4)$_{2n}$ (entries 6 and 7 in Table 4), and also with that of [Ag$_2$($C_9H_8NO_3$)$_2$(H_2O)$_2$]·2H_2O ($C_9H_8NO_3$ = *N*-acetylanthranilate, entry 5 in Table 4).[16b] The centrosymmetric dimers formed by two carboxylates and two silver(I) ions have been also reported in the silver(I)−amino acid complexes such as *β*-alaninesilver(I) nitrate {[Ag(NH_3(CH_2)$_2$$CO_2$)]($NO_3$)}$_2$ (Ag−Ag distance 2.855(4) Å, O−Ag−O angle 161.6(8)°)[13c,d] and {[Ag(Hglygly)]NO_3}$_2$ (Ag−Ag distance 2.92 Å, O−Ag−O angle 160°).[13a]

(14) (a) Wells, A. F. *Structural Inorganic Chemistry*, 4th ed.; Oxford University Press: London, 1975; p 1015. (b) Bondi, A. *J. Phys. Chem.* **1964**, *68*, 441.

(15) There has been confusion in judging whether the d^{10}−d^{10} metal(I) interaction is bonding or nonbonding. (i) For example, as to the complex [Ag$_2$(dppm)$_2$(NO_3)$_2$] with an Ag−Ag distance 3.085(1) Å (entry 30 in Table 4),[18o] one reference assigns this as Ag−Ag interaction bonding,[17e] while others assign it as nonbonding.[18a,o] (ii) The metallic radii for silver and gold on the cubic close-packing structures of metallic silver and gold (both 12-coordinate) are both 1.44 Å,[14a] and the van der Waals radii for silver and gold have been reported to be 1.72 and 1.66 Å, respectively.[14b] However, many references concerning silver(I) complexes have usually used the metallic 12-coordinate silver radii (1.44 Å) as indicators of metal−metal bonding,[9] while almost all references concerning gold(I) complexes have used the van der Waals radii of gold (1.66 Å) as indicators.[7] Thus, there are relatively large differences 2.88−3.44 Å in indicators for silver and also 2.88−3.32 Å for gold. (iii) Regarding the heteroleptic compounds containing silver(I)−gold(I) bonds, what can we use as the reference distances? (iv) Dance has reported that 12-coordinate silver with no ligands is bonding with silver at 2.88 Å, while two-coordinate silver with anionic thiolate ligands is nonbonding with silver at the same distance.[8b,c] Thus, he pointed out that metal−metal separations in elemental (12-coordinate) metals are unsuitable as reference distances for isolated metal−metal single bonds between low-coordinate metal atoms and, therefore, evaluation of metal−metal distances as indicators of metal−metal bonding must be made with reference to the coordination number. Jansen has also discussed the d^{10}−d^{10} cations interaction mostly with regard to silver(I).[8a] The Ag−Ag distances within the aggregates are approximately constant, the shortest being ca. 2.80 Å (shorter than the 2.89 Å in metallic silver) and the longest not longer than 3.30 Å (i.e., less than the van der Waals diameter of 3.40 Å). The shortest Ag−Ag distance between d^{10} cations in compounds of silver(I) oxides lies below 3.00 Å. In the numerous coordination compounds of silver(I) he listed, the Ag−Ag contacts are of similar length to the interatomic distances in the elements themselves, i.e., among 2.733−2.942 Å. Further, it is noteworthy that, as found in Table 4, the Ag−Ag distances within the Ag−O bonding clusters with the same coordination number are shortest, and the softness of the donor atom coordinated to the silver(I) atom significantly influences the Ag−Ag distance. Thus, as far as the silver(I) complexes are concerned, the d^{10}−d^{10} interaction should be considered in a wider range than the usually used reference distance, 2.88 Å.

(16) (a) Huang, W.-Y.; Lu, L.; Chen, X.-M.; Mak, T. C. W. *Polyhedron* **1991**, *10*, 2687. (b) Smith, G.; Reddy, A. N. K.; Byriel, A.; Kennard, C. H. L. *Polyhedron* **1994**, *13*, 2425.

Table 4. Comparison of Silver(I)−Silver(I) Interactions and Distances (Å)[a]

entry	complexes	coordination nos. of Ag(I) atoms[b]	Ag(I)−Ag(I)	ref
		Ag−O Bonding Clusters		
1	$[Ag(hfa)(diglyme)]_2$	7 (8)	2.9226(10)[d]	18a
2	$[Ag_2(hfa)(O_2CCF_3)(diglyme)_2]$	6 (7)	2.9513(6)[d]	18a
3	$[Ag(LBA)\cdot H_2O]_n$	4 (5)	2.8472(11)[f]	18b
4	$[Ag_{10}(L^1)_{12}(OTf)_2(H_2O)_4](OTf)_8\cdot 4H_2O$	4 (6)	2.7704(14)−3.2952(14)[f]	17f
5	$[Ag_2(C_9H_8NO_3)_2(H_2O)_2]\cdot 2H_2O$	3 (4)	2.831(2)[e]	16b
6	$[Ag_2(Et_3Bet)_2(NO_3)_2]$	4 (5)	2.929(1)[d]	16a
7	$\{[Ag_2(Et_3Bet)_2](ClO_4)_2\}_n$	3 (4)	2.856(2)[d]	16a
8	$[Ag_2(Bet)_2(H_2O)_2(NO_3)_2]_n$	4 (5)	2.898(1)[e]	17a
9	$[Ag_2(pyBet)_2(ClO_4)_2]_n$	4 (5)	2.814(2)[e]	17a
10	$[Ag(pyBet)(NO_3)]_n$	3 (5)	3.011(1)[e]	17b
11	$[Ag_2(O_2CNMe_2)_2]$	3 (4)	2.837(2)[d]	18c
12	$[Ag(Hpyrrld)]_2$ (**3**)	3 (4), 2 (3)	2.9022(7)[f]	c
13	$[Ag(S\text{-othf})]_2$	3 (4)	2.823(1)[f]	6i
14	$[Ag_2(S\text{-othf})(R\text{-othf})]$	3 (4)	2.781(1)[f]	6i
		Ag−N Bonding Clusters		
15	$\{[Ag(2,4'\text{-bpy})]ClO_4\}_n$	3 (4)	3.1526(6)[f]	18d
16	$\{[Ag(4,4'\text{-bpy})]NO_3\}_n$	2 (3)	2.78(2)−2.9696(20)[f]	18e,f
17	$[Ag_3(NC_5H_4CO_2H\text{-}4)_2]BF_4$	2 (4)	2.969(5)−3.236(5)[f]	18g
18	$\{[Ag(Him)_2]ClO_4\}_6$	2 (3), 2 (5)	3.051(1)[f]	18u
19	$\{[Ag(bpp)]OTf\}_n$	2 (3)	3.089(1)[e]	10d
20	$[C_6H_4O_2(Me_2SiN^tBu)_2]_2Ag_4$	2 (4)	2.990(2)−3.018(2)[d]	18h
		Ag−S Bonding Clusters		
21	$[(^tBuO)_3SiSAg]_4$	2 (4)	3.117(13)−3.153(7)[d]	18i
22	$[Ag(SR)]_6$	3 (5)	2.882(3)−3.279(2)[d]	18j
		Ag−Te Bonding Clusters		
23	$[(C_6H_5)_4P]_2[Ag_4(TeC_4H_3S)_6]$	3 (6)	av. 3.13(9)[e]	18k
		Ag−(O, N) Bonding Clusters		
24	$[Ag_2(C_5H_4NCO_2)]_n$	3 (4)	3.035(1)[e]	16b
		Ag−(S, P) Bonding Clusters		
25	$[Ag_4(SPh)_4(PPh_3)_4]$	4 (5)	3.1300(3)[f]	18l
		Ag−(N, P) Bonding Clusters		
26	$\{[Ag_2(MeCN)_2(\mu\text{-}L^2)](ClO_4)_2\}_n$	3 (4)	3.005(2), 3.184(2)[e]	17c
27	$\{[Ag\{HC(PPh_2)_3\}_2](ClO_4)_3\cdot 2MeCN\}_n$	2 (4)	3.1618(5)−3.2228(9)[e]	18m
28	$[Ag_2(\mu\text{-}L^3)_2(MeCN)_2](ClO_4)_2$	3 (4)	3.029(1)[d]	17d
		Ag−(O, S) Bonding Clusters		
29	$\{[Ag_4(hfa)_4(SEt_2)]\}_n$	4 (5)	3.046(2)[e]	18n
		Ag−(O, P) Bonding Clusters		
30	$[Ag_2(dppm)_2(NO_3)_2]$	4 (5)	3.085(1)[d]	18o
31	$[Ag_2(hfa)_2(dmpm)_2]$	4 (5)	3.153(1)[d]	18p
		Ag−(C, O) Bonding Clusters		
32	$[Ag_2(hfa)_2(cod)_2]$	7 (8)	2.955(2)[d]	18q
33	$[Ag_2(hfa)_2(dmcod)_2]$	4 (5)	3.0134(3)[d]	18r
		Ag−(O, N, P) Bonding Clusters		
34	$[Ag(\mu\text{-}L^4)(OTf)]_2$	3 (4)	3.033(1)[e]	17e
35	$[Ag_3(dppp)_2(MeCN)_2(ClO_4)_2]ClO_4$	3 (4), 2 (4)	2.943(2)−3.014(2)[e]	18s
		Ag−(S, Cl) Bonding Clusters		
36	$\{[Ag_8(\mu_4\text{-}SC_2H_4NH_3)_6Cl_6]Cl_2\}_n$	3 (6)	2.994(3)−3.046(3)[d]	18t
		Ag−(P, Cl) Bonding Clusters		
37	$[Ag_4Cl_4(dppm)_2]$	3 (5)	3.254(1)−3.374(1)[d]	18j

[a] hfa = hexafluoropentanedionato; LBA = D-lactobionato; L^1 = (4-(dimethylamino)pyridino)acetato; 2,4′-bpy = 2,4′-bipyridine; 4,4′-bpy = 4,4′-bipyridine; $NC_5H_4CO_2H$-4 = isonicotinic acid; bpp = 1,3-bis(4-pyridyl)propane; RSH = 6-(*tert*-butyldimethylsilyl)pyridine-2-thione); $C_5H_4NCO_2$ = pyridine-3-carboxylato-(*O*,*O*′); L^2 = 3,6-bis(diphenylphosphino)pyridazine; L^3 = (2-diphenylphosphino-6-pyrazol-1-yl)pyridine; dppm = bis(diphenylphosphino)methane; dmpm = bis(dimethylphosphino)methane; cod = 1,5-cyclooctadiene; dmcod = dimethyl-1,5-cyclooctadiene; L^4 = 1-[(diphenylphosphino)methyl]-4-(2-pyridyl)piperazine; dppp = bis(diphenylphosphino)phenylphosphine. [b] Excluding Ag(I)−Ag(I) bonds (including Ag(I)−Ag(I) bonds). [c] This work. [d] Reported as nonbonding. [e] Not referred to bonding or nonbonding. [f] Reported as bonding.

Solution (^{109}Ag, ^{1}H, and ^{13}C) NMR. Solution molecular weight measurements have indicated that **1** is present as a dimer in solution. The ^{109}Ag NMR spectrum in D_2O of **1** as a single peak at 476 ppm showed that two silver(I) ions in this dimeric complex were equivalent, as well two Hhis$^-$ ligands. This ^{109}Ag chemical shift is much more shifted to higher field, compared with those of related silver(I) complexes, e.g., $[Ag(1,2,3\text{-triz})(PPh_3)_2]_n$ at 994 ppm ($CDCl_3$),[6c] $[Ag(1,2,4\text{-triz})(PPh_3)_2]_n$ at 925 ppm ($CDCl_3$),[6c] $[Ag(im)(PPh_3)_3]$ at 1186 ppm ($CDCl_3$),[6b] $\{Na[Ag(Htma)]\cdot 0.5H_2O\}_n$ at 868.7 ppm (D_2O),[6e] $\{Na[Ag(mba)]\cdot H_2O\}_n$ at 855.6 ppm (D_2O),[6f] and $[Ag(Hmba)(PPh_3)_3]\cdot CH_2Cl_2$ at 1196 ppm ($CDCl_3$).[6h] In the last three silver(I) complexes, the coordination to the silver(I) atom is completed with sulfur and/or phosphorus donor atoms and, in their complexes, the carboxyl oxygen donor atom does not participate in the coordination.

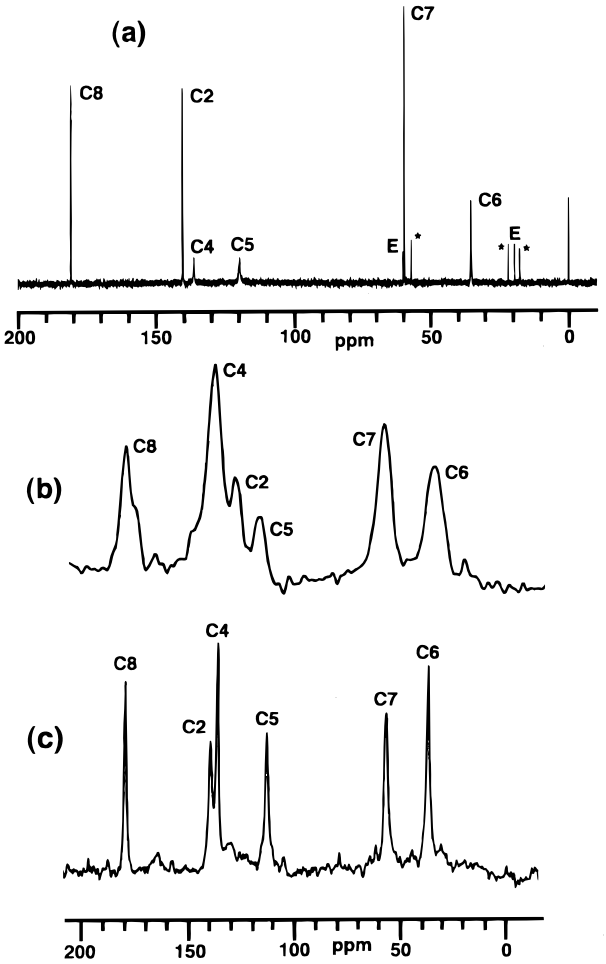

Figure 5. (a) ^{13}C NMR spectrum in D_2O at 25 °C of **1**, (b) solid-state ^{13}C NMR spectrum at 24.1 °C of **1**, and (c) solid-state ^{13}C NMR spectrum at 24.8 °C of **2**. In (a), the carbon signals denoted by asterisks are from methylene groups of the internal reference DSS and the carbon signals denoted by E are from solvated EtOH.

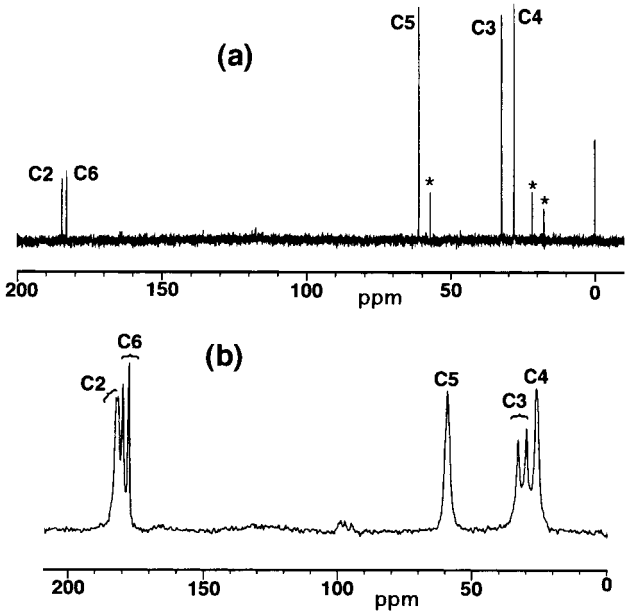

Figure 6. (a) ^{13}C NMR spectrum in D_2O at 25 °C of **3** and (b) its solid-state ^{13}C NMR spectrum at 24.4 °C. In (a), the carbon signals denoted by asterisks are from methylene groups of the internal reference DSS.

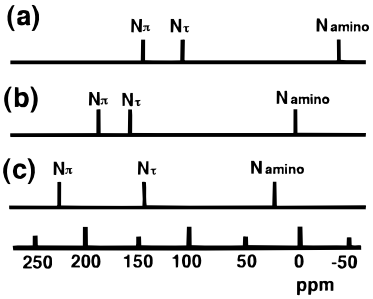

Figure 7. (a) Solid-state ^{15}N NMR chemical shifts, with reference to an external NH_4NO_3, at 24.5 °C of **1**, (b) at 24.7 °C of **2**, and (c) at 25.0 °C of the free H_2his ligand.

The ^1H NMR spectrum in D_2O of **1** showed signals of the coordinating $Hhis^-$ ligand observed as a doublet of doublets (H7; four lines) of a vicinal proton of a methyne group, two double doublet (H6; four lines × 2) signals of geminal protons of the neighboring methylene group, and H2 and H5 protons within the imidazole ring, as well as signals from EtOH solvated. The ^{13}C NMR spectrum in D_2O of **1** (Figure 5a) was a six-line spectrum consisting of C6, C7, and C8 signals and C2, C4, and C5 signals within the imidazole ring, in addition to signals based on EtOH solvated, where the quaternary carbons C4 and C8 were assigned on the basis of the off-resonance method. These chemical shifts are shown in the Experimental Section.

On the other hand, the ^{109}Ag NMR spectrum in D_2O of **3** could not be measured, because an aqueous solution with sufficient concentration cannot be prepared even by elevating the temperature. The ^1H NMR spectrum in D_2O of **3** showed signals of the coordinating $Hpyrrld^-$ ligand as multiplet peaks of two methylene groups (H4 and H3) and a double doublet (four lines) of the H5 proton within the ring. The ^{13}C NMR spectrum in D_2O of **3** (Figure 6a) was a five-line spectrum consisting of C3, C4, C5, C2, and C6 signals, each as a single peak, showing two $Hpyrrld^-$ ligands in the dimeric form of **3** equivalent in solution.

Solid-State (^{13}C and ^{15}N) NMR. The solid-state ^{15}N and ^{13}C NMR measurements have shown that the silver(I) histidinate complex is present as two different polymers in the solid state, i.e., the water-soluble powder **1**, $\{[Ag(Hhis)]_2\}_n$, with a dimeric core and the water-insoluble crystals $[Ag(Hhis)]_n$ (**2**) without a core complex.

The solid-state ^{15}N NMR spectra measured at room temperature of the free H_2his ligand and the two complexes **1** and **2** were composed of all three-line spectrum due to the N_{amino} atom and the N_τ and N_π atoms in the imidazole ring, and their signals were assigned on the basis of the literature (Figure 7).[19] In **2** (Figure 7b), only two signals of the N_{amino} and N_π atoms were shifted to higher field by the complexation; the shift observed was ca. 18 ppm for the N_{amino} atom and ca. 36 ppm for the N_π atom, whereas the N_τ atom was ca. 10 ppm shifted to *lower* field, compared with the H_2his ligand (Figure 7c). X-Ray crystallography has revealed that the bonding mode of **2** consists of a 2-coordinate silver(I) atom that is bonding only with the N_{amino} and N_π atoms in the two different $Hhis^-$ ligands,

(17) (a) Chen, X.-M.; Mak, T. C. W. *J. Chem. Soc., Dalton Trans.* **1991**, 1219. (b) Chen, X.-M.; Mak, T. C. W. *Polyhedron* **1991**, *10*, 1723. (c) Kuang, S. M.; Zhang, Z.-Z.; Wang, Q. G.; Mak, T. C. W. *Chem. Commun.* **1998**, 581. (d) Kuang, S.-M.; Zhang, L.-M.; Zhang, Z.-Z.; Wu, B.-M.; Mak, T. C. W. *Inorg. Chim. Acta* **1999**, *284*, 278. (e) Kuang, S.-M.; Zhang, Z.-Z.; Wang, Q.-G.; Mak, T. C. W. *Inorg. Chem.* **1998**, *37*, 6090. (f) Wei, P.; Mak, T. C. W.; Atwood, D. A. *Inorg. Chem.* **1998**, *37*, 2605.

respectively, but not with the N_τ atom. This fact is consistent with the observed solid-state ^{15}N NMR spectra of **2**.

On the other hand, all three ^{15}N signals of **1** were remarkably shifted to higher field (Figure 7a). The shift observed by the complexation was ca. 60 ppm for the N_{amino} atom and ca. 78 ppm for the N_π atom, while that of the N_τ atom was ca. 37 ppm. Probably, the water-soluble powder **1** is a polymer with a dimeric core in the solid state, namely, $\{[Ag(Hhis)]_2\}_n$, where the bonding to the silver(I) center is accomplished with the N_{amino} and N_π atoms, and the polymerization takes place through intermolecular hydrogen bonding between the CO_2^- group and the N_τ atom of the dimeric cores. The higher field shift of the N_τ atom will be attributed to the hydrogen-bonding interaction.

The solid-state ^{13}C NMR spectra of **1** measured in the temperature range of 24 to 140 °C were composed of very broad signals, supporting its polymeric nature in the solid state (the ^{13}C NMR spectrum measured at 24.1 °C is shown in Figure 5b and variable-temperature solid-state ^{13}C NMR data are provided in the Supporting Information). Compared with solution ^{13}C NMR (Figure 5a), it should be noted that the C2 carbon peak in the solid state is shifted to higher field, ca. 12.6 ppm. Since the numbers of the carbon resonances in the solid state are identical with those in solution, i.e., both being six-line spectrum, two Hhis ligands in the dimeric core in **1** in the solid state are equivalent. The quaternary carbons C4 and C8 were assigned on the basis of the ^{13}C MASDL method. The sample measured at 140.0 °C was cooled and remeasured after 2 h at 25.0 °C. In comparison with the starting sample, the C5, C2, and C8 carbon signals were significantly shifted to higher field (ca. 0.5−0.8 ppm).

On the other hand, **2** has shown ^{13}C NMR spectral patterns different from those of **1** (the solid-state ^{13}C NMR spectrum measured at 24.8 °C is shown in Figure 5c): (i) The variable-temperature solid-state ^{13}C NMR was composed of much sharper signals than those of **1** but much broader than the solution ^{13}C NMR of **1**. (ii) The chemical shifts of C4 and C2 carbons were interchanged, in which the quaternary carbon C4 was also assigned on the basis of the ^{13}C MASDL method. (iii) No significant ^{13}C NMR change took place in the temperature range between room temperature and 140 °C. (iv) All carbon signals of the sample remeasured at 25.0 °C, after once measured at 140.0 °C, were almost identical with those of the starting sample within the range of 0.1−0.2 ppm.

Solid-state and solution ^{13}C NMR measurements of **3** show that two coordinating Hpyrrld$^-$ ligands are unequivalent in the solid state as substantiated by X-ray crystallography, while they are equivalent in solution. In fact, compared with solution ^{13}C NMR (Figure 6a), solid-state ^{13}C NMR signals of C2, C3, and C6 were observed as two peaks, respectively (Figure 6b), reflecting the presence of two unequivalent Hpyrrld$^-$ ligands in the solid state. The C4 and C5 resonances, found as a single peak, may be insensitive to such unequivalent environments. All ^{13}C chemical shifts in the solid state were broadened and shifted to higher field. These spectral patterns were also found in the elevated temperature up to 140 °C. Probably, no significant structural change takes place in the temperature range between room temperature and 140 °C. On the other hand, solid-state ^{15}N NMR of **3** measured at 24.0 °C showed only one ^{15}N resonance as a very broad peak at 72.3 ppm. As observed in the C4 and C5 carbon resonances, the nitrogen resonance at this position in the heterocycle may be insensitive to the two different environments of the Hpyrrld$^-$ ligands.

Antibacterial and Antifungal Activities. Antimicrobial activities of **1**−**3**, together with those of **4** and **5**,[6a] are listed in Table 5, as estimated by minimum inhibitory concentration (MIC; μg mL^{-1}).

Antimicrobial activities of the free ligands, H_2his and H_2-pyrrld, were estimated as >1000 μg mL^{-1} for bacteria, yeast, and mold and, thus, showed no activity. The Ag^+ ion, as aqueous $AgNO_3$, has shown remarkable activities against Gram-negative bacteria (*E. coli*, *P. aeruginosa*), moderate activities against one Gram-positive bacteria (*B. subtilis*), and no activity (>1600 μg mL^{-1}) against 2 yeasts and 10 molds.[6a] The complex **3**, on the contrary, showed remarkable and excellent activities against a wide spectrum of Gram-negative and -positive (*B. subtilis* and *S. aureus*) bacteria and yeast (*C. albicans* and *S. cerevisiae*) and even against many molds except *A. niger* and *A. terreus*. A similar wide spectrum was also obtained in **1**. The complex **2** showed a wide spectrum of modest activities. Of particular note is the fact that in **1** and **3** activities against many molds are observed. These activities mostly correspond to those of the previous silver(I)−N bonding complexes **4** and **5**.[6a] Thus, the two difficulties in the practical application, namely, the water insolubility of **4** and the light instability of **5** were improved by the finding of **1** and **3**. The modest activities of **2** cannot be simply attributed to its low solubility in water, because both **4** and **5** show effective activities despite quite different solubilities in water.

Studies of the mechanism of antimicrobial activities by silver(I) complexes have been scarcely reported, although three possible mechanisms for inhibition by the aqueous silver(I) ion have been proposed: (i) interference with electron transport; (ii) binding to DNA; (iii) interaction with the cell membrane.[2a] We have so far suggested that the ease of ligand replacement in silver(I)−N bonding compounds appears to be one of the key factors leading to a wide spectrum of effective antimicrobial

(18) (a) Darr, J. A.; Poliakoff, M. Blake, A. J.; Li, W.-S. *Inorg. Chem.* **1998**, *37*, 5491. (b) Kim, K. M.; Song, S. C.; Lee, S. B.; Kang, H. C.; Sohn, Y. S. *Inorg. Chem.* **1998**, *37*, 5764. (c) Alessio, R.; Dell'Amico, D. B.; Calderazzo, F.; Englert, U.; Guarini, A.; Labella, L.; Strasser, P. *Helv. Chim. Acta* **1998**, *81*, 219. (d) Tong, M.-L.; Chen, X.-M.; Ye, B.-H.; Ng, S. W. *Inorg. Chem.* **1998**, *37*, 5278. (e) Robinson, F.; Zaworotko, M. J. *J. Chem. Soc., Chem. Commun.* **1995**, 2413. (f) Yaghi, O. M.; Li, H. *J. Am. Chem. Soc.* **1996**, *118*, 295. (g) Burrows, A. D.; Mahon, M. F.; Palmer, M. T. *J. Chem. Soc., Dalton Trans.* **1998**, 1941. (h) Veith, M.; Woll, K. L. *Chem. Ber.* **1993**, *126*, 2383. (i) Wojnowski, W.; Wojnowski, M.; Peters, K.; Peters, E.-M.; v. Schnering, H. G. *Z. Anorg. Allg. Chem.* **1985**, *530*, 79. (j) Perez-Lourido, P. A.; Garcia-Vazquez, J. A.; Romero, J.; Louro, M. S.; Sousa, A.; Chen, Q.; Chang, Y.; Zubieta, J. *J. Chem. Soc., Dalton Trans.* **1996**, 2047. (k) Zhao, J.; Adcock, D.; Pennington, W. T.; Kolis, J. W. *Inorg. Chem.* **1990**, *29*, 4358. (l) Ahmed, L. S.; Dilworth, J. R.; Miller, J. R.; Wheatley, N. *Inorg. Chim. Acta* **1998**, *278*, 229. (m) Che, C.-M.; Yip, H.-K.; Yam, V. W.-W.; Cheung, P.-Y.; Lai, T.-F.; Shieh S.-J.; Peng, S.-M. *J. Chem. Soc., Dalton Trans.* **1992**, 427. (n) Xu, C.; Hampden-Smith, M. J.; Kodas, T. T.; Duesler, E. N.; Rheingold, A. L.; Yap, G. *Inorg. Chem.* **1995**, *34*, 4767. (o) Ho, D. M.; Bau, R. *Inorg. Chem.* **1983**, *22*, 4073. (p) Yuan, Z.; Dryden, N. H.; Vittal, J. J.; Puddephatt, R. J. *Can. J. Chem.* **1994**, *72*, 1605. (q) Bauley, A.; Corbitt, T. S.; Hampden-Smith, M. J.; Kodas, T. T.; Duesler, E. N. *Polyhedron* **1993**, *12*, 1785. (r) Dopplet, P.; Baum, T. H.; Ricard, L. *Inorg. Chem.* **1996**, *35*, 1286. (s) Che, C.-M.; Yip, H.-K.; Li, D.; Peng, S.-M.; Lee, G.-H.; Wang, Y.-M.; Liu, S.-T. *J. Chem. Soc., Chem. Commun.* **1991**, 1615. (t) Su, W.; Cao, R.; Hong, M.; Chen, J.; Liu, J. *Chem. Commun.* **1998**, 1389. (u) Eastland, G. W.; Mazid, M. A.; Russell, D. R.; Symons, M. C. R. *J. Chem. Soc., Dalton Trans.* **1980**, 1682.

(19) (a) Kawano, K.; Kyogoku, Y. *Chem. Lett.* **1975**, 1305. (b) Levy, G. C.; Lichter, R. L. *Nitrogen-15 Nuclear Magnetic Resonance Spectroscopy*; John Wiley: New York, 1979; p 74. (c) Alei, M., Jr.; Morgan, L. O.; Wageman, W. E.; Whaley, T. W. *J. Am. Chem. Soc.* **1980**, *102*, 2881. (d) Gooley, P. R.; Johnson, B. A.; Marcy, A. I.; Cuca, G. C.; Salowe, S. P.; Hagmann, W. K.; Esser, C. K.; Springer, J. P. *Biochemistry* **1993**, *32*, 13098. (e) Chen, Y.-L.; Park, S.; Thornburg, R. W.; Tabatabai, L. B.; Kintanar, A. *Biochemistry* **1995**, *34*, 12265.

Table 5. Antibacterial and Antifungal Activities of **1**−**3**, and the Related Silver(I)−N-Containing Heterocycle Complexes **4** and **5** Evaluated by Minimum Inhibitory Concentration (MIC: μg mL^{-1})

test organisms	$[Ag(Hhis)]_2$ (**1**)	$[Ag(Hhis)]_n$ (**2**)	$[Ag(Hpyrrld)]_2$ (**3**)	$[Ag(im)]_n$[a] (**4**)	$[Ag(Him)_2]NO_3$[a] (**5**)
Escherichia coli	15.7	125	7.9	6.3	7.9
Bacillus subtilis	62.5	250	31.3	50	15.7
Staphylococcus aureus	62.5	250	15.7	50	15.7
Pseudomonas aeruginosa	15.7	250	7.9	12.5	7.9
Candida albicans	15.7	125	7.9	50	15.7
Saccharomyces cerevisiae	15.7	125	7.9	<3.2	15.7
Aspergillus niger	125	250	500	50	15.7
Penicillium citrinum	500	250	250	6.3	15.7
Aspergillus terreus	500		1000	12.5	
Rhizopus stolonifer	62.5		15.7	6.3	
Chaetomium globosum	15.7		7.9	12.5	
Cladosporium cladosporioides	15.7		7.9	12.5	
Penicillium islandicum	31.3		15.7	12.5	
Aureobasidium pullulans	31.3		7.9	25	
Fusarium moniliforme	31.3		31.3	25	
Eurotium tonophilum				6.3	

[a] Reference 6a.

activities and the primary targets for the inhibition of bacteria and yeast by **4** and **5** are proteins as sulfur donor ligands and not nucleic acids as N/O donors.[6a,b] Thus, it is reasonable that **1** and **3** with the weaker bonds such as Ag−N and Ag−O bonds, respectively, show a wider spectrum of antimicrobial activities, because the further ligand replacement with biological ligands is possible.

Conclusions

The bonding modes of **1**−**3** in the solid state, represented as $\{[Ag(Hhis)]_2\}_n$, $[Ag(Hhis)]_n$, and $\{[Ag(Hpyrrld)]_2\}_n$, respectively, are noteworthy. Not only in the structural viewpoint but also in the biological viewpoint, **3** occupies a special position, because of both the helicity and the aurophilic interaction and its remarkable antimicrobial activities. In the silver(I) complexes, metal(I)−metal(I) interaction has been discussed in ref 15. The title complexes are also of interest as a possible new type of solid-state inorganic polymer; efforts toward X-ray analysis studies using *R*- and *R*,*S*-forms of H_2pyrrld and their related ligands are continuing and will be reported in due course.

Acknowledgment. We thank Professor Wasuke Mori, Department of Materials Science, Kanagawa University, Hiratsuka, Japan, for his assistance in the X-ray measurements using the imaging-plate diffractometer. Also, we thank Akito Sasaki, Rigaku Co., Tokyo, Japan, for useful discussion of the crystal data.

Supporting Information Available: X-Ray crystallographic files, in CIF format, and text providing variable-temperature solid-state ^{13}C NMR data for compounds **1**−**3**. This material is available free of charge via the Internet at http://pubs.acs.org.

IC990526O